Swiss J Palaeontol (2016) 135:125–138
DOI 10.1007/s13358-015-0096-8

Interpreting drag consequences of ammonoid shells by comparing studies in Westermann Morphospace

Kathleen A. Ritterbush[1,2]

Received: 27 February 2015 / Accepted: 9 July 2015 / Published online: 5 October 2015
© Akademie der Naturwissenschaften Schweiz (SCNAT) 2015

Abstract Differently-shaped ammonoid shells present varied hydrodynamic properties, but the relevance of shell shape to ammonoid paleoecology is unclear. To examine trends in ammonoid shell shape that relate to hydrodynamic consequences, we project ammonoid shell data into Westermann Morphospace. Operationally similar to other multivariate methods, Westermann Morphospace features a fixed frame and scaling calibrated around the most common planispiral morphotypes. First, results of hydrodynamic experiments are projected into the space, to test for associations between recognized morphotypes and measures of drag force. Discocone shell shapes produce minimal drag at small sizes and/or low speeds, while oxycone shells produce minimal drag at higher sizes and/or faster speeds. If hydrodynamic efficiency was a first-order selective pressure on shell shapes produced by ammonoids, an association is expected between larger adult shells and oxyconic geometry. To assess this, published shape data are shown in Westermann Morphospace to examine intervals of evolutionary interest. A rough analysis of Late Triassic ammonoid shell shapes shows the expected association between larger shells and oxyconic geometry, but the association is completely reversed immediately after the end-Triassic mass extinction, and the association does not return among the "recovered" middle Jurassic ammonoids. This suggests that hydrodynamics suited for high-metabolism rapid locomotion were not a first-order influence on shell shape immediately after the extinction, or that other hydrodynamic influences require assessment by different methods. Lastly, shells of a series of endemic chronospecies of Cretaceous *Neogastroplites* are compared, showing a shift to inclusion of more discoconic shells at smaller sizes, resulting in minimal drag for more of the ontogenetic series as a whole. Together, these results indicate that size must be considered when interpreting the hydrodynamic efficiency of ammonoid shells. Flank shape, ornament and soft tissue behaviors may be as or more important than first-order shell geometry, and quantification of their importance and influence on varied shell geometries will benefit from further experimental results.

Keywords Mass extinction · Functional morphology · Evolution · Paleobiology · Morphometrics · Mesozoic

Introduction

Variations in ammonoid shell shape have apparent hydrodynamic consequences, which have been studied theoretically and experimentally. Buoyancy, stability, and interference with water flow all relate to shell geometry, size, speed, position, ornamentation, suture complexity, and propulsion dynamics (e.g., Chamberlain 1976; Chamberlain and Westermann 1976; Saunders and Shapiro 1986; Jacobs 1992; Elmi 1993; Jacobs et al. 1994; Westermann 1996; Olóriz et al. 2002; Klug and Korn 2004; Hammer and Bucher 2006). Morphometric studies vary in their relevance to paleoecological interpretation by directly or indirectly examining shell shape parameters that relate to specific hydrodynamic consequences. Simplification of multidimensional shape data onto composite agnostic axes without prior expectations is

✉ Kathleen A. Ritterbush
k.ritterbush@utah.edu

[1] Department of the Geophysical Sciences, University of Chicago, 5734 S Ellis Ave, Chicago, IL 60637, USA

[2] Present Address: Department of Geology and Geophysics, University of Utah, 115 S 1460 E, Salt Lake City, UT 84112, USA

well suited for open-ended explorations of shell shape evolution within specific ammonoid groups or samples (e.g., Dommergues et al. 1996; Yacobucci 2004; McGowan 2004). The morphospaces that result from multivariate techniques are typically sensitive to the shell data employed, and are thus not directly comparable between studies, either visually or statistically. Plotting shell data along generation axes is helpful for understanding ontogenetic processes and shell constructional constraints (e.g., Raup 1967; Smith 1986; Klug and Korn 2004; Monnet et al. 2011b). One way to test ecological interpretations of shell shape is to use morphospaces with functional axes that attempt to summarize shape parameters of known hydrodynamic influence (Monnet et al. 2011a; Ritterbush and Bottjer 2012).

Westermann Morphospace combines three parameters in a fixed frame (traits of Raupian space) with a multidimensional projection (similar to PCA but impervious to changes in the dataset analyzed; see Fig. 1). In addition, the display can be scaled to interrogate the variation between recognized ammonoid morphotypes. Westermann (1996) produced an intuitive framework of continuous variation between major ammonoid morphotypes, along with interpretations of shell mobility (see also Westermann and Tsujita 1999). Ritterbush and Bottjer (2012) expressed the morphospace quantitatively by plotting data according to the relative proportions of three shape parameters (umbilical exposure, overall inflation, and whorl expansion; see "Methods", below). It is now necessary to explore how well different combinations of these parameters do indeed relate to shell hydrodynamics. Here, hydrodynamic properties of shells spanning the morphospace are analyzed in two ways: first, to determine if individual shape parameters influence hydrodynamics as expected; second, to determine if and how specific suites of parameters influence hydrodynamics. The latter result addresses the value of using a morphospace designed to quantify Westermann's observed framework. Westermann Morphospace also provides a fixed frame for simple visual comparison of hydrodynamic results to collections of specimens from interesting evolutionary intervals in Earth history.

Hydrodynamic studies examined

Chamberlain (1976) designed pioneering hydrodynamic experiments on model ammonoid shells, producing a suite of quantitative results across a spectrum of shapes. He produced 37 plexiglass models of ammonoid shells of uniform diameter (12.7 cm) and varied umbilical diameters and whorl heights. On every model, the whorl width was equal to its height, thereby maintaining a constant of the whorl aspect ratio S, which is critical in Raup's (1967) logarithmic growth model. Drag was measured by moving each shell model through a water tank at a fixed speed (10–250 cm/s; Reynolds numbers 12,500–312,500), and water flow around each model was visualized using dyes in a separate flume tank. Replicate experiments placed each shell with an adjusted aperture angle position. Chamberlain discussed the variation in measured drag as a function of speed (and Reynolds number) and as a factor of variation in the shell geometry. The shell shapes observed to produce the least drag have been interpreted as adaptive peaks in evolution that are still invoked today to explain ammonoid paleoecology (Smith et al. 2014).

Jacobs' (1992) experiments further scrutinized the hydrodynamic consequences of two additional aspects of shell shape, as well as the importance of size. First Jacobs tested the importance of thickness ratio which varied widely among Chamberlain's models but was not addressed specifically. Jacobs produced fiberglass casts of real fossil shells expressing varied overall shell compression (4 compressed, 2 inflated, 5 intermediate). Second, Jacobs addressed a critical artifact of shell models as experimental subjects. Whereas sharp aperture terminations of Chamberlain's models produced eddies of water flow that may have been altered by the presence of animal soft tissue (Chamberlain 1980), Jacobs added a simple clay taper to the edge of each fossil cast to mimic a minimally exposed soft body. Finally, Jacobs targeted changes in drag with changing locomotion speed by moving small shell models (3.5–5.77 cm diameter) at speeds of 0–50 cm/s (Reynolds numbers <30,000). Jacobs compared measured drag force to overall Reynolds number for each specimen, and discussed how combinations of size and speed could affect locomotion costs.

Morphospace studies examined

Ammonoid shell shape data published with each of two thorough morphometric studies are shown in Westermann Morphospace to explore the expression of ammonoid morphotypes at intervals of particular evolutionary interest. Specifically, results of the hydrodynamic studies are compared to the shape studies to determine if there is any evidence for the selective pressure to the reduction of shell drag. Reduction of shell drag is an extremely general concept that could be coincident with phylogenetic or constructional constraints (such as Cope's rule; see discussion in Monnet et al. 2011a, b for ammonoids specifically, as well as Hone and Benton 2005) or could be a result of selective pressure working on vastly different scales; from a broad influence across space and time, to a particular consequence of local environmental and ecological interactions acting on a single population. (Smith et al. 2014).

The first study examines the shells made by different taxa from around the world throughout very large time intervals crossing a mass extinction boundary. Morphology and ecology of Late Triassic to Early Jurassic ammonoids

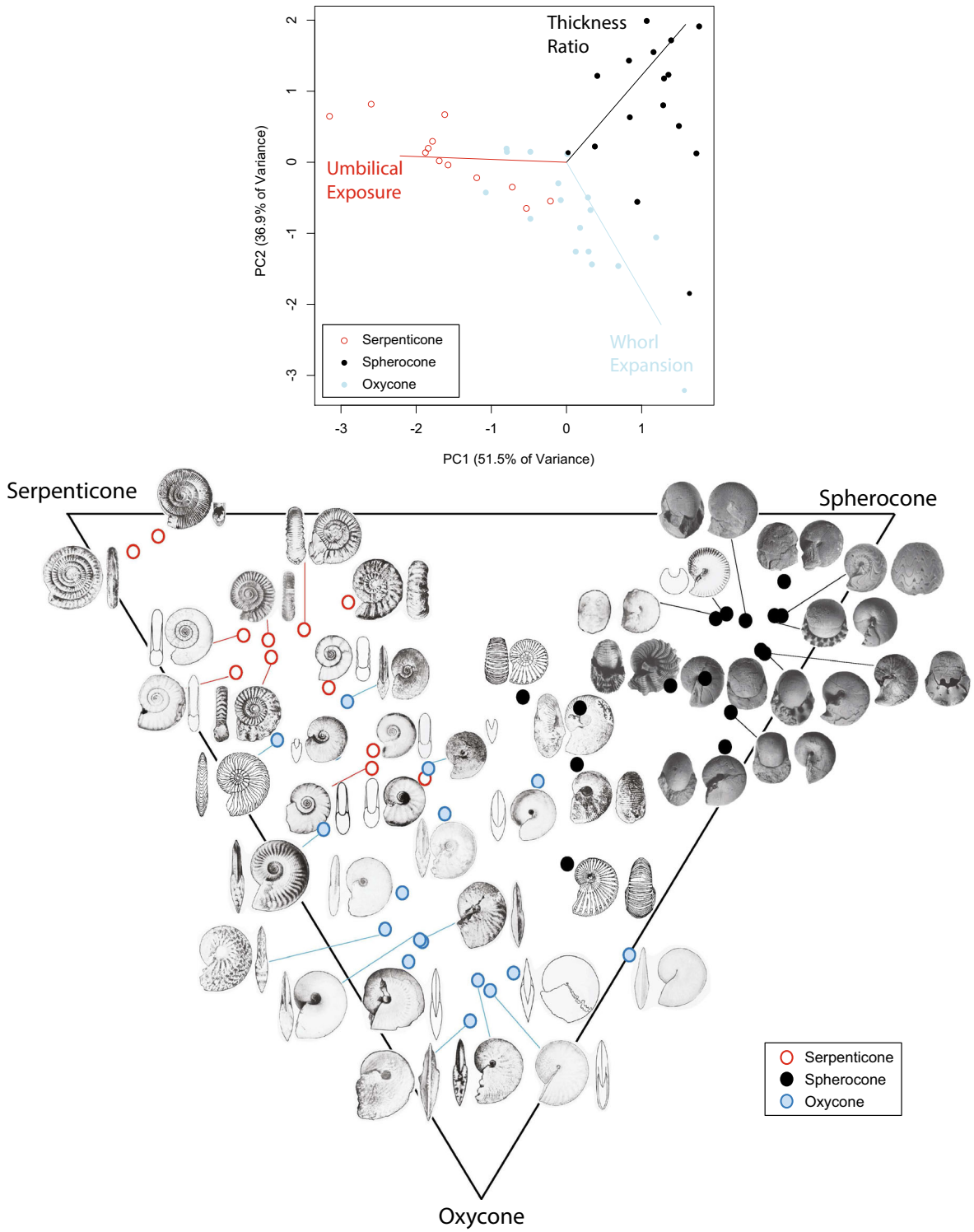

Fig. 1 Serpenticone, oxycone, and spherocone shells from the *Treatise* (Arkell et al. 1957; Selden 2009) shown in principle components analysis (PCA; *top graph*) and Westermann Morphospace (*lower graph*). The first two PCA axes assess 88.4 % of the variation in three variables (represented by *vectors*). PCA projects the data across a plane that maximizes the visualization of their variation, but this plane shifts as data are added or removed from analysis. Arrangement of these data is similar in Westermann Morphospace, in which scaling calibrates even distribution of the three morphotypes at opposing ends of a *triangular diagram*. The frame does not shift when data are added, removed, or compared between studies. Images from the *Treatise* show the variation of shapes across the space. See Ritterbush and Bottjer (2012) for data and for elaboration on the method. Parameter loadings for principle components axis one are −44 % umbilical exposure (*U*), 25 % whorl expansion (*w*), and 31 % thickness ratio (Th). Axis 2 2.1 % *U*, −53 % *w*, 45 % Th. Axis 3 (not shown): 39 % *U*, 29 % *w*, 32 % Th

have been assessed in detail by myriad studies (e.g., Smith and Tipper 1986; Guex 1995; Dommergues et al. 1996, 2001; Dera et al. 2010; Simon et al. 2011), with a compilation of shape data recently published by Smith et al. (2014). Smith et al. (2014) compiled measurements from literature of one specimen per geologic stage (Carnian to Callovian; 235–161 Mya) from each of 682 genera (successfully covering 60–90 % of all genera that occurred in each stage). They then compared the shell shape data in Raupian theoretical morphospace, and used adaptive peaks from Chamberlain (1976, 1981) to designate geologic stage intervals as representing ammonoids of Pre-extinction, Aftermath, Post-extinction and Recovery morphologic disparity and potential paleoecology. Westermann's highlighted morphotypes were also included for reference on the Raupian space (Smith et al. 2014; Fig. 9), and here Smith et al.'s compiled size and shape data are directly shown in Westermann Morphospace to compare with hydrodynamic results from both size and shape experiments.

The second study examines intraspecies variation in a single seaway over a very short time interval. Yacobucci (2004) compared shell shape variation within each chronospecies of *Neogastroplites* from the Cretaceous Mowry Sea, spanning 1.5–1.8 Myr. Yacobucci examined intraspecies shape variation using both linear measurements and discriminant analysis of natural logs of shell measurements, which produced an ordinated morphospace custom to the specimens under investigation. Yacobucci determined that, after introduction of a second ammonoid species/population into the seaway, *Neogastroplites* intraspecies shape variation remained high but included a new shell shape unconstrained by previous shape parameter correlations. Here Yacobucci's detailed analysis is also projected into Westermann Morphospace, to examine the novel *Neogastroplites* shells in the context of hydrodynamic data.

The results of all four above studies were compared in Westermann Morphospace to test if evolutionary intervals of interest produced ammonoid shells with apparently persistent first-order hydrodynamic consequences. The results of Chamberlain (1976) and Jacobs (1992) are compared to determine the conditions and caveats accompanying interpreted "adaptive peaks". The intervals of shell shape variation featured in Smith et al. (2014) and Yacobucci (2004) are examined for any coincident expression of these "adaptive peaks". Considering both shape and size of the fossil shells allows quantification of the speeds at which hydrodynamic consequences would introduce potentially relevant trade-offs in locomotion efficiency. Overall, such analyses can support or reject interpretations of hydrodynamic efficiency as a contributing selective pressure, and can indicate more specific tests for future work.

Methods

Projecting shell data into Westermann Morphospace can be executed simply using spreadsheet software or via an available R package. Three ratios are required from each shell: umbilical exposure (as a proportion of diameter); whorl expansion over the most recent 180° of shell accretion; and overall inflation (aperture width as a ratio over diameter). These parameters best assess the outermost first-order shape of the final shell, without regard to the theoretical growth process that attained it (Ritterbush and Bottjer 2012). Each ratio is scaled relative to common ammonoid shells (taken from Raup 1967; Arkell et al. 1957; Selden 2009). For each specimen, three scaled values are divided by their sum to determine relative contributions to overall shell shape. The relative contributions by each parameter are plotted in a ternary diagram.

A ternary diagram juxtaposes three mutually exclusive values. While extents of raw shape parameters are not mutually exclusive in ammonoids' flexible growth mechanism, the relative contribution of each parameter to final shape characterization is mutually exclusive. As in the original observational scheme drawn by Westermann, data placement varies according to the relative proportions of the three morphotypes, rather than raw individual values. For reference, Fig. 1 shows shells identified as serpenticones, oxycones, or spherocones in the Treatise (Arkell et al. 1957; or globlular shells from Selden 2009; see Korn 2010). These morphotype terms can refer to specific traits (e.g., platycones can be characterized as serpenticonic or oxyconic because they are both evolute and compressed) but are retained here, as in Westermann (1996), to label the opposing corners of the morphospace (whereas other terms better fit the intermediate shells; platycone, discocone, cadicone, planorbicone, etc.). Figure 1 shows the data both in a principal components analysis (PCA; executed with function prcomp in R; R Core Team 2013) and Westermann Morphospace. In either method, a plotted point can be inverted to solve for a relative proportion of shape characteristics that fit a narrow variety of exact shapes. The frame of Westermann Morphospace is fixed by the scaling employed (if any), and is not sensitive to the amount or type of shell data displayed within it. Scaling is not required, but here we use a scaled morphospace to focus on the area between recognized morphotypes, because that is most relevant to our fossil and hydrodynamic data. In this case extreme values (shells with final negative whorl expansion or thickness ratio below 14 %) are displayed as such, outside the frame that houses typical and exaggerated ammonoid shell values (see Ritterbush and Bottjer Fig. 3). This projection method does not alter the underlying data or the statistical relationships between datasets.

Measurements of model and fossil shell shapes reported in Chamberlain (1976) and Jacobs (1992) were used to plot the shapes in Westermann Morphospace (Ritterbush and Bottjer 2012) and theoretical morphospace (Raup 1967). Coefficients of drag were noted from tables in Chamberlain (1976) and read from scatter plots (Jacobs 1992; Fig. 5) with open source image analysis software (ImageJ). Jacobs' drag data were fit with semilog least-squares regressions using open source statistical analysis software (R Core Team 2013). Hydrodynamic properties (coefficients of drag and slopes of drag coefficients) were then compared to basic shell shape parameters and to the Westermann Morphospace axis values (percent on each ternary axis that determines closeness to the serpenticone, oxycone, or spherocone corner of the morphospace). Hypotheses based on previous work were tested: (1) Coefficients of drag should be significantly associated to variation in one or more parameters that contribute to Westermann Morphospace, in a way that depends on size. For example, in shells greater than 1 cm diameter, increased drag is expected on ammonoid shells with larger thickness ratio values. (2) Coefficients of drag should be significantly associated with Westermann Morphospace axis values. For example, in shells greater than 1 cm diameter, increased drag is expected for ammonoid shells that have a relatively large thickness ratio, and a small umbilical exposure, and a small whorl expansion. In this example, the combination of traits places the shell in the "sphereocone" portion of the morphospace. Do hydrodynamics correspond to the relative suites of parameters that set Westermann's morphotypes apart? Correlations were assessed with Spearman's rho, an estimate of association between ranked variables (using open source programming language R; R Core Team 2013) and illustrated in figures with contour plots generated using the MASS (Venables and Ripley 2002; Akima 2013) and Westermann Morphospace (Ritterbush and Bottjer 2012) packages.

Next, ammonoid shell shape data from both Smith et al. (2014) and Yacobucci (2004) are examined in Westermann Morphospace, as well as with principle components analysis (R Core Team 2013) and theoretical morphospace (Raup 1967). Specimens yielding usual shell parameter values ($w > 2.2$, $w < 0$, thickness ratios <0.14) were examined and verified ($n = 3$), remeasured ($n = 12$) or excluded pending monograph availability ($n = 22$), resulting in 746 specimens representing 667 genera. Hydrodynamic variables from the above studies were compared to shape variables in the fossil studies using open source statistical software (R Core Team 2013). Unless otherwise noted, reported Spearman's rho values are for $p < 0.05$.

Results

Hydrodynamics

Drag measures from Chamberlain's model experiments

The reported coefficients of drag for each shell model shape are contoured in Westermann Morphospace in Fig. 2. Figure 2a shows results for shells with the aperture in "rest" position, adjusted for the shells individually, and Fig. 2b shows results for shells with the apertures each positioned at a 30° angle. Drag coefficient is an estimate of the drag that is a consequence of shape alone, rather than speed and size. For comparison, a 1-cm sphere moving 1 cm/s will have a coefficient of drag of exactly 1, which will be slightly lower at higher Re. In both cases, the models producing the lowest drag coefficient are marked by filled circles. One is somewhat serpenticonic shape and the other is a spherocone. The measured coefficients of drag increase dramatically as the models plot lower in the

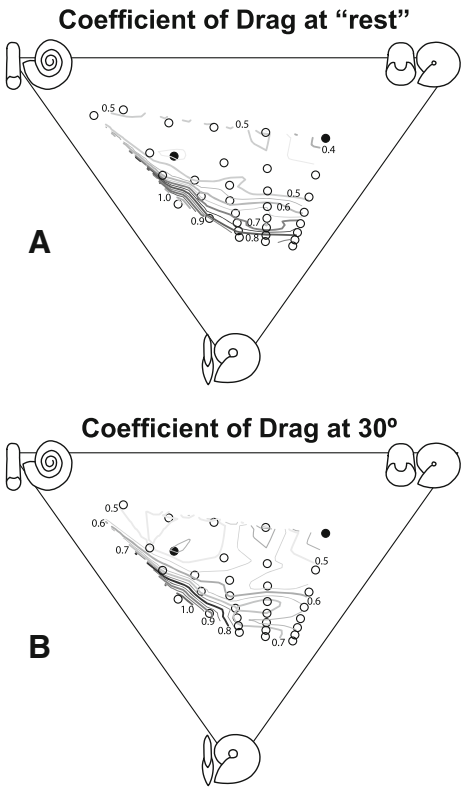

Fig. 2 The relative shapes of ammonoid shell models tested by Chamberlain (1976) are shown in Westermann Morphospace (*circles*). Reported measured coefficients of drag are represented in each diagram with contoured isolines. **a** Coefficients of drag reported for models in "rest" position, with unique aperture angles designated for each shell (see Chamberlain 1976; Table 1). **b** Coefficients of drag reported for models each positioned at 30°. *Filled circles* in both **a** and **b** mark the shell models with the lowest reported drag

morphospace to approach the oxycone corner, with the platycone position along the lower left flank of the diagram yielding the highest measures (Spearman $\rho = 0.73$ at "rest" and 0.61 at 30°, both $p < 0.001$). The contribution of umbilical exposure to overall shell shape was associated with higher drags on models at "rest" position (Fig. 2a; nearness to the serpenticone corner has a $\rho = -0.37$, $p = 0.030$). When all shells are positioned with the aperture at 30° (Fig. 2b), the variation in drag is more complex, particularly with respect to the sphereocone axis representing the relative importance of inflation.

Drag measures from Jacobs shape and speed experiments

Image and shape data from the fossil specimens used in Jacobs' (1992) experiments are represented in Westermann Morphospace in Fig. 3. Experimental data read from Jacobs (1992) are plotted on one semilog graph in Fig. 4, with significantly fitted least-squares trend lines. Jacobs noted that the slope with which drag changes over speed is strongly significantly correlated to the overall inflation (thickness ratio; whorl width over diameter) of the specimens. As expected, the drag slopes also show a large

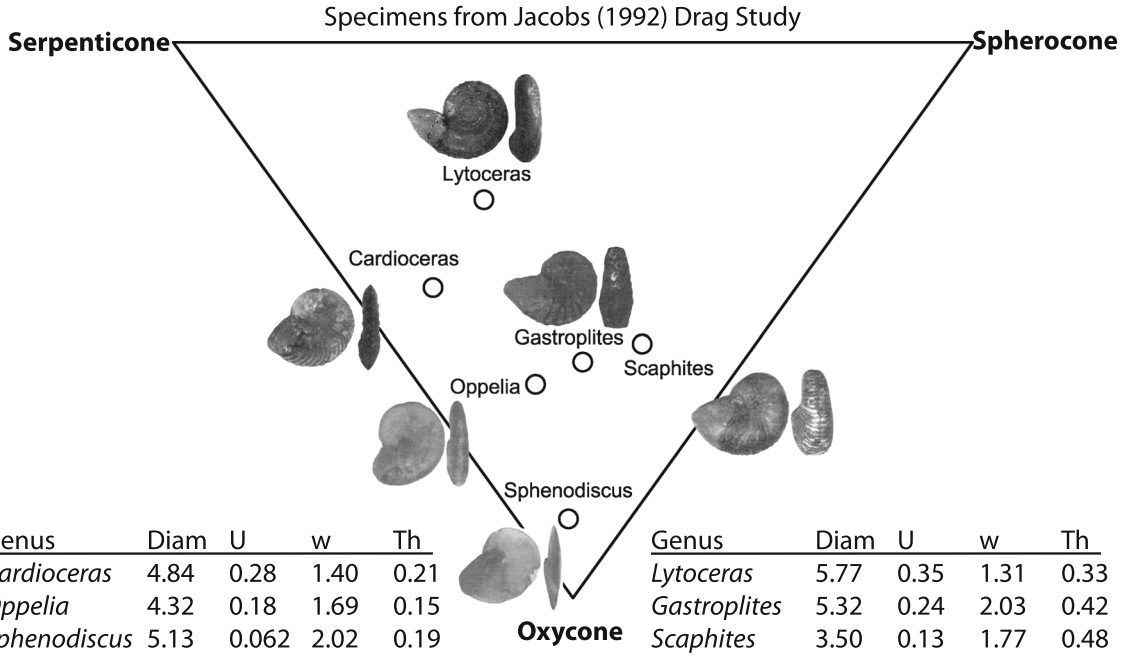

Genus	Diam	U	w	Th
Cardioceras	4.84	0.28	1.40	0.21
Oppelia	4.32	0.18	1.69	0.15
Sphenodiscus	5.13	0.062	2.02	0.19

Genus	Diam	U	w	Th
Lytoceras	5.77	0.35	1.31	0.33
Gastroplites	5.32	0.24	2.03	0.42
Scaphites	3.50	0.13	1.77	0.48

Fig. 3 Six ammonoid specimens with published coefficients of drag from Jacobs (1992) are plotted in Westermann Morphospace (*circles*) alongside genus names and specimen images. Diameters and shape ratios from each shell are included

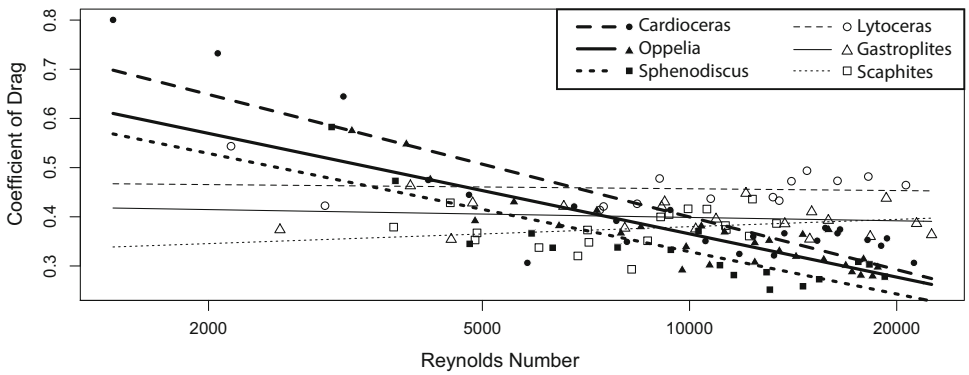

Fig. 4 Coefficients of drag measured on six casts of fossil shells by Jacobs (1992) are plotted against the log of tested Reynolds number (Re). Least-squares regression lines are shown for each specimen. The more streamlined shells (Cardioceras, Oppelia, Sphenodiscus) produce the highest drag coefficients at Re < 3400, but produce the lowest drag coefficients at Re > 11,200. Regression lines for specimens with similar involution across around Re = 7000 (Cardioceras should produce less drag than Lytoceras when Re = 6816; Sphenodiscus should produce less drag than Scaphites when Re = 7050; Oppelia should produce less drag than Gastroplites when Re = 7515)

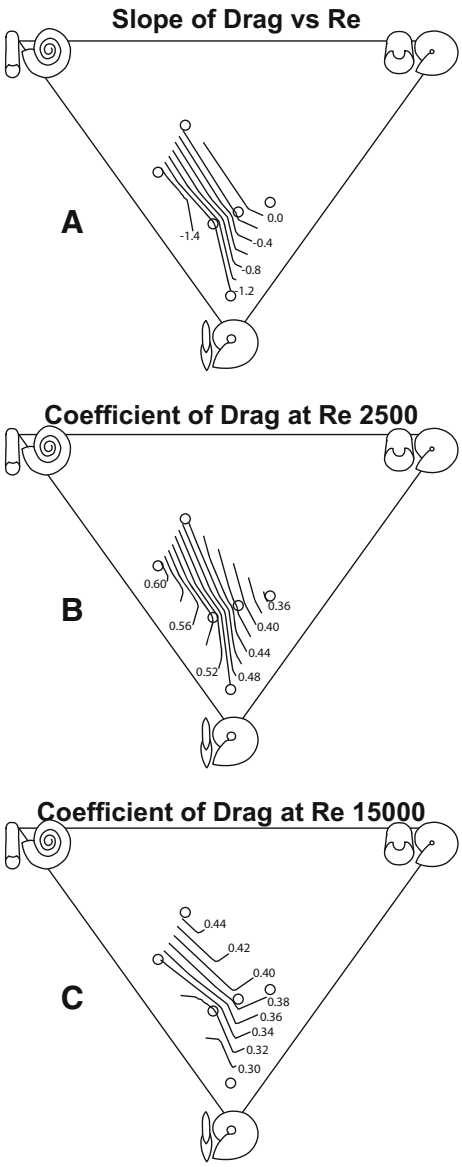

Fig. 5 Jacobs' (1992) hydrodynamic results for six ammonoid shell specimens are shown in Westermann Morphospace. **a** The slope for the line fitted to coefficient of drag and Re (Fig. 4) are contoured onto Westermann Morphospace. **b** Contours for coefficient of drag at Re 2500. Note the shift to higher drag measures as shells plot farther from the spherocone corner. **c** Contours for coefficient of drag at Re 15000. Note the shift to lower coefficients of drag as shells plot closer to the oxycone corner

association with the specimen placement within Westermann Morphospace (Fig. 5; Spearman $\rho = 0.83$, $p = 0.029$). Inflated forms plotting closer to the spherocone region are associated with neutral or positive drag/Re slopes, whereas more compressed forms (note that *Cardioceras*, *Oppelia*, and *Sphenodiscus* all plot close to the left leg of the diagram; Fig. 3) show negative slopes, because drag decreases dramatically at higher Re (Fig. 5a).

More importantly, Jacobs discovered trade-offs in hydrodynamic efficiency. At low Re, compressed forms produce more drag than inflated forms (Fig. 4). At high Re, compressed forms produce less drag than inflated forms (Fig. 4). As could be predicted from Jacobs' conclusions, at Re 2500—suitable for ammonoids with 5-cm shells traveling one shell length per second—shells plotting closer to the spherocone corner have lower drag estimates (Fig. 5b). At Re 1500—suitable for ammonoids with a 10-cm shell traveling one and a half-shell length per second—shells plotting closer to the spherocone corner have higher drag estimates (Fig. 5c). Figure 5 further demonstrates important associations between drag and the two other main parameters of shell shape. Among the compressed specimens of very similar thickness ratio, *Cardioceras* has the largest umbilical exposure and the lowest whorl expansion while *Sphenodiscus* has the smallest umbilical exposure and highest whorl expansion (see measures in Fig. 3). This causes them to fall nearly in a line along the left leg of Westermann Morphospace. Coincidentally, the drag of the same three shells decreases with increasing whorl expansion and decreasing umbilical exposure (Fig. 4). Similarly, the specimens of *Lytoceras*, *Gastroplites*, and *Scaphites* show decreasing drag (Fig. 4) as whorl expansion increases and umbilical exposure decreases. Beyond comparing drag to the individual shape parameters, we can take advantage of the scaled percent values of Westermann Morphospace which summarize the relative contribution of each parameter to overall shell morphotype. Based on shell shapes described above, increasingly oxyconic forms should have the lowest drags when high Re are considered. As illustrated in Fig. 5c at Re 15,000, there is a large negative association (Spearman $\rho = -0.77$, $p = 0.051$) between drag and placement near the oxycone corner of the space (summarized by the % oxycone in the morphospace plotting axes). This relationship is absent at the very low Re, where inflation is the dominant variable (Fig. 5b), and the lowest drag occurs in the discoconic *Scaphites*. The breakdown of the relationship at low Re is clear when viewing Fig. 4: at low Re, the triplet of compressed forms with decreasing drag (and increasing oxycone form) overly the triplet of inflated forms with increasing drag (and increasing discocone form), so the only overall relationship is to the relative closeness to the sphereocone space (Spearman' $\rho = 0.77$; $p = 0.051$). In contrast, at high Re shells nearer the spherocone region have higher drag (Spearman' $\rho = 0.77$; $p = 0.051$).

Case studies

Late Triassic–Middle Jurassic

Ammonoids produced profoundly different suites of shell shapes across the Late Triassic to middle Jurassic interval, and the differences in overall morphotype representation are clear in Westermann Morphospace (Fig. 6). In the Pre-

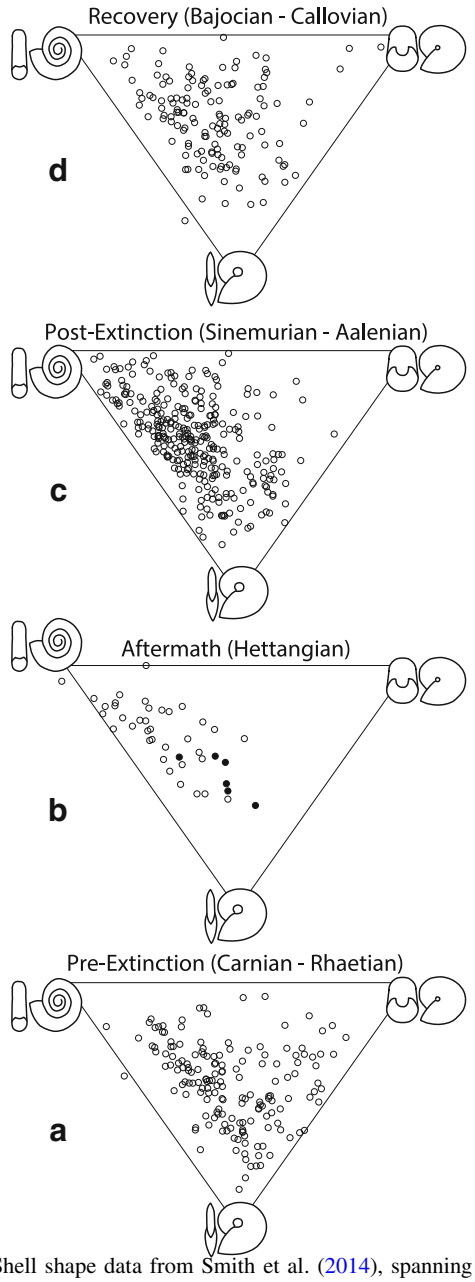

Fig. 6 Shell shape data from Smith et al. (2014), spanning the Late Triassic to Middle Jurassic are shown in Westermann Morphospace. Designations of stages into "Pre-Extinction", "Aftermath", "Post-Extinction", and "Recovery" intervals following the interpretations of Smith et al. (2014). **a** "Pre-Extinction" ammonoid faunas from the Late Triassic (Carnian—Rhaetian; ~34 Myr) represented by 166 specimens of 151 genera. A Carnian specimen of *Pompeckjites* has a thickness ratio of 13 %, causing it to plot just outside the focus morphospace. **b** "Aftermath" ammonoids from the Hettangian (~1.8 Myr; Schaltegger et al. 2008; Schoene et al. 2010) stage of the Early Jurassic represented by one specimen from each of 42 genera. A specimen of *Laqueoceras* has a thickness ratio of 11 %, causing it to plot just outside the focus morphospace. **c** "Post-Extinction" ammonoids of the Sinemurian—Aalenian (~28 Myr) represented by 301 specimens from 271 genera. **d** "Recovery" ammonoids from the remaining Middle Jurassic (Bajocian—Callovian; ~11 Myr) represented by 138 specimens of 137 genera. A Callovian specimen of *Petitclercia* has a thickness ratio of 12 %, causing it to plot just outside the focus morphospace

Extinction interval (Triassic stages Carnian, Norian, Rhaetian; Fig. 6a), ammonoids produced shells with uncorrelated variations of all three parameters (central area of the morphospace is well filled), with additional oxyconic and discoconic shapes. In the Aftermath of the extinction (Jurassic Hettangian stage; Fig. 6b), the new psiloceratid ammonoid clade produced particularly serpenticonic shells. Several of the more involute and inflated shells were produced by the Phylloceratoidea (filled circles in Fig. 6b; from upper right to lower left: *Paradasyceras, Togaticeras, Geyeroceras, Phylloceras, Nevadaphyllites, Fergusonites*). During the Post-Extinction interval (Sinemurian, Pliensbachian, Toarcian, and Aalenian; Fig. 6c), ammonoids produced shells of both definitively serpenticonic and definitively oxygenic morphotypes. Save for a lower frequency and extremity of spherocones, the shell shapes produced in the Early Jurassic nearly recapture the breadth of the Pre-Extinction ammonoids. Finally, during the Recovery interval (Bajocian, Bathonian, Callovian; Fig. 6d), the most extreme examples of each morphotype were produced, expanding the morphospace from the Pre-Extinction observations. The frequency of representation among the different shapes is more sparse and even.

Only the Pre-Extinction shells expressed hypothesized associations between size and shape. There is a small significant association between shell diameter and oxycone geometry ($\rho = 0.22$, $p = 0.0019$). This is matched by a congruous negative correlation between diameter and serpenticone geometry ($\rho = 0.23$, $p = 0.0011$). Within the Pre-Extinction ammonoid specimens, shells plotting ≥60 % in the oxycone corner (median size 32.3 mm) are larger than those plotting ≥60 % in the serpenticone corner (median size 54.0 mm; Wilcoxon rank sum test $p = 0.052$). In the immediate extinction aftermath (Hettangian stage, approximate duration 1.6 Myr; Schoene et al. 2010; Schaltegger et al. 2008), the size distribution is entirely reversed, with the larger ammonoid shells forming serpenticones ($\rho = 0.41$; $p = 0.0038$). This association remains positive but decreases in importance during the Post-Extinction ($\rho = 0.15$; $p = 0.0045$) and Recovery ($\rho = 0.14$; $p = 0.050$) intervals. The median shell size increased significantly from the Pre-Extinction to Hettangian intervals (medians of 33.5 and 45.9 mm, respectively; Wilcoxon Rank Sum $p < 0.001$), with particularly dramatic change among serpenticones (32.3 and 85.4 mm, respectively; Wilcoxon rank sum $p = 0.0022$). Shells sizes at all quantiles across all morphotypes continued to increase through the Post-Extinction and Recovery stages and, though the stage-to-stage increases are not all significant during the Early and Middle Jurassic, shells at each interval were significantly larger than those of the Pre-Extinction interval (Fig. 7).

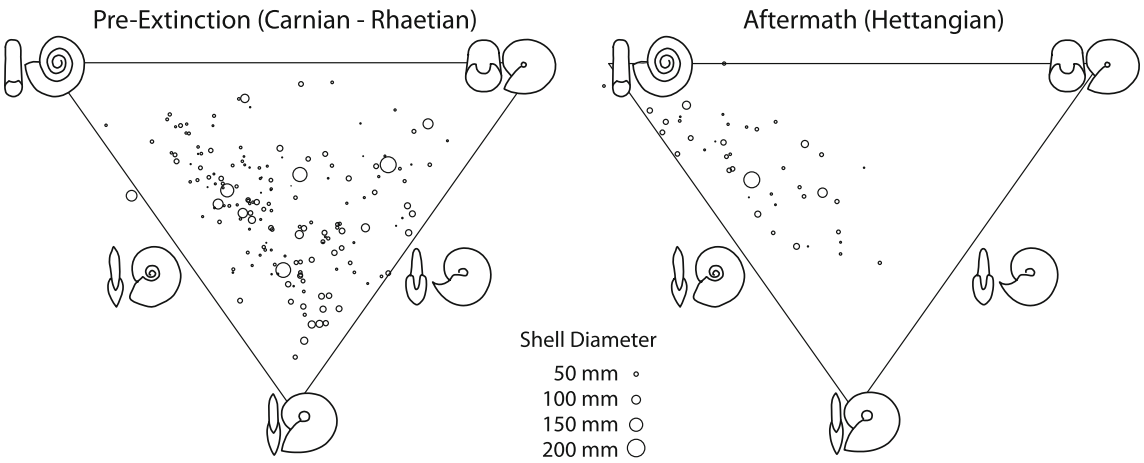

Fig. 7 Ammonoid shell shape data in Westermann Morphospace for Late Triassic (*left*) and Early Jurassic (*right*; Hettangian only). Data are the same as Fig. 6a, b, with the size of each *symbol* representing the diameter of the corresponding specimen (see key)

Late Cretaceous Mowry sea

Projection in Westermann Morphospace shows that *Neogastroplites* shells varied chiefly between oxycones and cadicones (Fig. 8). *Neogastroplites* was initially represented by discoconic and oxyconic specimens of *N. Haasi*, then by chiefly oxyconic shells of *N. cornutus*. After the arrival of *Metengonoceras*, represented by rare specimens among the *N. cornutus* and more common specimens among the *N. muelleri* and *N. americanus* (Yacobucci 2004), each successive *Neogastroplites* chronospecies included less oxyconic shells than *N. cornutus*, and grew to include cadicone shells. Figure 9 contrasts shell diameter to each of the critical shape parameters. In each chronospecies, larger shells are strongly associated with reduced umbilical exposure (rho varies from −0.46 to −0.63). Whorl expansion shows a moderate association with shell diameter only in *N. americanus* ($\rho = 0.34$). An overall association of reduced inflation at higher diameters ($\rho = -0.41$) is due to *N. cornutus*, *N. muelleri*, and *N. americanus* (rho of −0.42 to −0.52). A general association between diameter and plotting along the oxycone axis ($\rho = 0.20$) disappears when *N. americanus* are removed from the data.

Discussion

Illustrating the results of hydrodynamic experiments in Westermann Morphospace supports interpretations presented by Westermann (1996). Drag does not respond to raw shape parameters in a vacuum; rather, drag changes dynamically as suites of parameters form specific morphotypes. For example, Jacobs (1992) demonstrated that drag increases on inflated shells (thickness ratio, or aperture width as a fraction of diameter). Westermann's (1996) expectation of low hydrodynamic efficiency for sphereocones specifically addresses shells with not only a high inflation, but additionally low umbilical exposure and low whorl expansion rate. Indeed, drag measures change dramatically in shells with a higher percent shape characterization by inflation, which plot closer to the "sphereocone" corner of Westermann Morphospace (Fig. 5b). Similarly, Westermann presented oxycones, shells with high whorl expansion and low umbilical exposure and inflation, as the most efficient shapes. Shells that plot closer to the "oxycone" corner of Westermann Morphospace have a higher percentage of shape characterization attributable to the whorl expansion, and Fig. 5c demonstrates that the greater the percent of shape characterization by whorl expansion, the less the drag in Jacobs' experiments. Overall, the oxyconic and discoconic forms are producers of minimal drag at high and low Re, respectively.

The comparisons of hydrodynamic data highlight critical trade-offs, as consequent drag for different morphotypes is altered when the influences of different parameters combine at different sizes or speeds. The strong reduction in drag for oxycones disappears at lower Re, as inflation becomes more influential (Fig. 5b, c). Jacobs (1992) addressed this phenomenon as a difference between the behavior of compressed shells, and we see here that the trends have influence beyond variation of a single parameter, to the full variety of morphotypes presented by Westermann (1996). The comparisons presented also highlight critical differences between the experimental results of Chamberlain (1976) and Jacobs (1992), that stem from a glitch in model design. Chamberlain discussed that a covered umbilicus should limit turbulence, and that overall shell compression should cause order of magnitude decreases in drag, yet in Chamberlain's experiments, shell models with higher whorl expansions produced excessive drag despite covered umbilici. This occurred because the

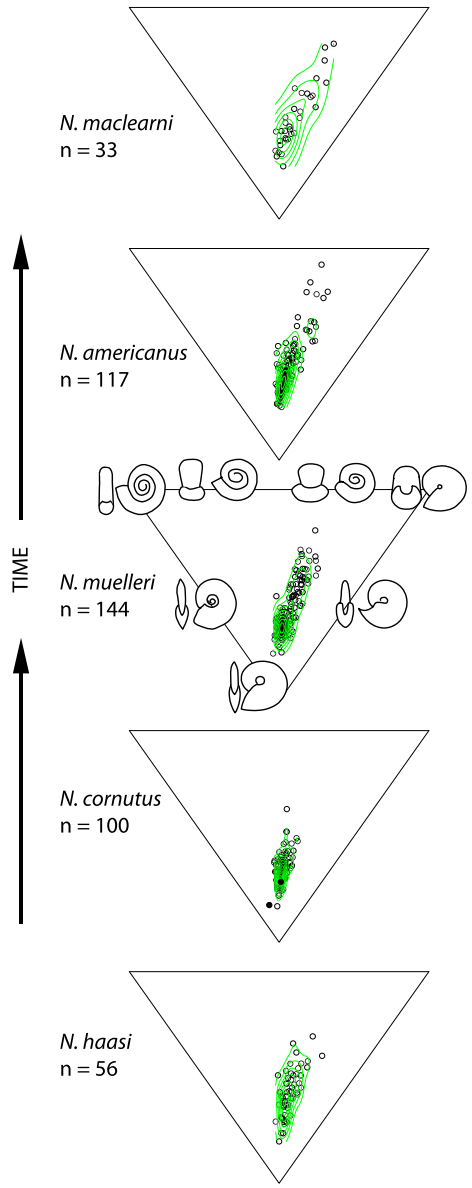

Fig. 8 Shell shape data from Yacobucci (2004) for fossils of five chronospecies of *Neogastroplites* from the Cretaceous Mowry Sea displayed in Westermann Morphospace. Contours show density of specimens in the morphospace. Two specimens of *Metengonoceras* are represented with *filled circles* in the diagram of *N. cornutus*

shells all had aperture aspect ratios (*S*) equal to 1, so the models with the largest whorl expansion consequently had the largest exposed flat aperture surfaces at the rear of the moving form, producing excess drag that would not occur on a living animal. Chamberlain acknowledged this and concluded that at least in overall compressed shells, the oxycone forms with high whorl expansion should produce the least drag and allow the maximum possible swimming velocities (Chamberlain 1981). By testing shells more representative of typical ammonoids, and by adding a taper

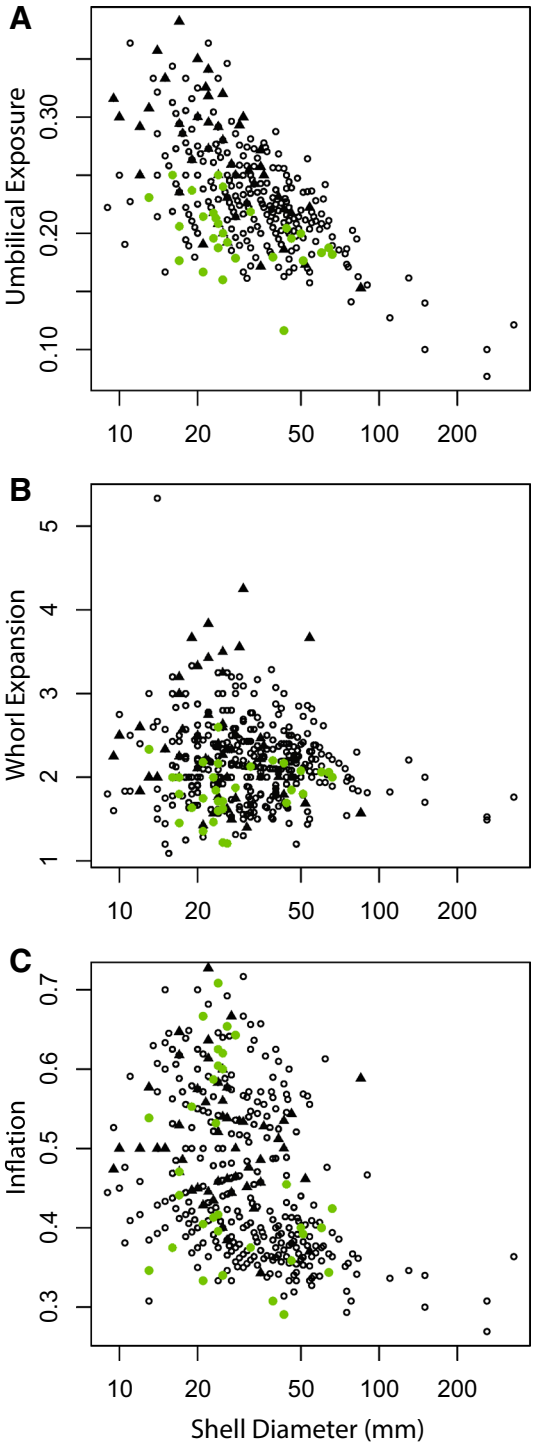

Fig. 9 Shell shape parameters of shells of all *Neogastroplites* specimens included in Yacobucci (2004), calculated following Ritterbush and Bottjer (2012). *Triangles* indicate the first chronospecies, *N. haasi*. *Filled circles* indicate the final chronospecies, *N. maclearni*. Note that whorl expansion (**b**) is the observed expansion of the aperture at a half-whorl rotation, rather than the asserted logarithmic expansion. Values of all three variables are significantly higher in *N. haasi*, though the difference is most apparent in umbilical exposure (**a**) and whorl expansion (**b**)

to mimic minimally exposed soft tissue, Jacobs' experiments do indeed yield the expected result, that a compressed shell with high whorl expansion and low umbilical exposure does produce lower drag (at decent sizes and/or speeds). As presented in Fig. 5c, this satisfies Westermann's interpretation.

Jacobs' experiments support Westermann's interpretations and demonstrate that the "adaptive peaks" based on Chamberlain's models are not representative of minima of drag production in shells generally. One interpretation of Jacob's data is that ecological or environmental pressures favoring decreased drag might result in oxycone shells being more frequent in larger ammonoids, and in the evolution of possible physiological accommodations for brief rapid jet propulsion. More experiments are needed to better test the hydrodynamic consequences of variation between shell morphotypes. Though based on few shells, Jacobs' hydrodynamic results produce a surprisingly coherent variation across Westermann Morphospace, suggesting an overarching framework that may persist through more detailed experiments. The three parameters of Westermann Morphospace capture only first-order shell shape, and ignore a wide variety of properties that also influence hydrodynamics and overall performance as a vessel in water (ornamentation, suture form, buoyancy, shell texture; e.g., Chamberlain and Westermann 1976; Olóriz et al. 1997, 2002; Elmi 1991, 1993). Further experiments can determine conditions in which additions of ornamentation override or reverse the trends demonstrated here. Most important to the study of ammonoid ecology, a possible function of a shell does not demonstrate that it was a necessary function, or that it was accompanied by tandem evolution of adequate musculature and physiology. Cases of high intraspecies variation are particularly interesting because they produce a record of animals that survived to adulthood in a variety of shell shapes and must have had overall very similar soft tissues. To expand this discussion, one high-resolution study of the evolution of intraspecies variation is discussed further below.

Possible ecological consequences of the Triassic–Jurassic transition

Ammonoid shells in the Late Triassic include forms that could be expected to produce fairly low drags, including both discocones and oxycones. Immediately after the extinction, the vast majority of ammonoids produced serpenticonic shells, which are suspected to both produce higher drag forces and limited stability. Before the extinction, more streamlined oxyconic shells are generally larger than the ammonoid shells of less streamlined morphotypes, which could be associated with selective pressure for drag reduction. In the extinction aftermath, the elimination of hydrodynamic streamlined shells, and the very large size of the serpenticonic shells, suggests that hydrodynamics suited for high-metabolism rapid locomotion were not a first-order influence on shell shape production in the earliest Jurassic. Guex has interpreted iterative ammonoid shell morphology as a passive consequence of Cope's rule of increasing body size (Guex 2003; see also Monnet et al. 2011a, b), and the Hettangian plethora of serpenticones (Guex 1995) as atavistic stress response of the entire regenerate clade (Guex 2001, 2006). Smith et al. (2014) show the radiation of Hettangian serpenticones coinciding with the low-drag adaptive peak in Chamberlain's (1976) results. Although Jacobs' data suggest this adaptive peak is not universal, the large cosmopolitan and ubiquitously abundant Hettangian psilocerids and offshoots may have been adroit passive ocean drifters with low metabolisms. Chamberlain and Westermann (1976) estimate that ornament increases efficiency at speeds above 15 cm/s, and Elmi (1991, 1993) demonstrates that the drag around ammonoid flanks, particularly evolute flanks, is dramatically impacted by ornamentation and by the shape of the overlying whorls that form the umbilical shoulder. Whether employed as a stress response or due to constructional constraint, the large smooth serpenticone shells of early Hettangian ammonoids may have allowed a fairly passive life mode. Quantifying the efficiency of slow propulsion in these shells benefits from additional consideration of the umbilical flank shape. The elaboration of serpenticones with dense high ribs and ornate venters may have imparted improved hydrodynamic efficiency to Sinemurian ammonoids without much overall change in the shell or soft tissue physiology, showcasing a condition in which ornament is more important than first-order shape (Elmi 1993).

It is possible to apply Jacobs' (1992) results to estimate the order of magnitude of speed at which Late Triassic ammonoids would need to have moved to gain any hydrodynamic advantage from their more streamlined shells. Pooling the Carnian—Rhaetian shell data, the median oxycone shells were about 5.4 cm in diameter, while the median serpenticone shells were about 3.3 cm in diameter. If moving 1.5 shell lengths per second, an ammonoid with a 5.4-cm oxycone shell could gain a 15 % reduction in drag compared to that expected if it had a smaller serpenticone shell. While a speed of 1.5 shell lengths per second might be unlikely for continuous swimming or long distance migration, sudden jet burst to dodge predators or capture prey are more likely scenarios. The ability to quantify what speeds would be required paves the way for more experiments and comparisons to modern cephalopod physiology and behavior.

Interpreting changes in *Neogastroplites*

Within a different ecological context, examination of Yacobucci's *Neogastroplites* data (2004) provides higher temporal resolution and includes ontogenetic change. Despite dramatic shell shape variation within each chronospecies of *Neogastroplites*, viewing the shells in Westermann Morphospace demonstrates that they chiefly grade between oxycones and cadicones. The change through time from oxycones to more discocones and cadicones after the arrival of *Metengonoceras* is easy to see, as is the lack of apparent influence of Buckman's law of covariation (see discussion in Yacobucci 2004), which would predict shells varying in the serpenticone to oxycone region of the morphospace. The way variation among individual shell parameters conspire to form shells of morphotypes we recognize is well illustrated between both Raupian theoretical morphospace (Fig. 9) and the Westermann Morphospace (Fig. 8). Specimens of the latest occurring chronospecies, *N. maclearni*, express about the same thickness ratios as the earliest *N. haasi*, but display lower whorl expansions and lower umbilical exposures. To cover more of the umbilicus without expanding the whorl results in a relatively smaller body chamber volume and a cadicone shape, the *N. maclearni* reach higher into the cadicone territory of Westermann Morphospace (Fig. 8) relative to *N. haasi*, but more importantly, even their discoconic forms are constructed by a fairly different means. Yacobucci (2004) discussed the variation in *Neogastroplites* as a product of a considerably plastic developmental framework. It can further be considered how any mode of selection might have favored the rise of discocones and cadicones after the introduction of *Metengonoceras* into the Mowry Sea.

Based on only the preliminary data from Jacobs (1992), it is possible to make some broad interpretations of the *Neogastroplites* shell shape change through time, and the importance of shell size. At a median size of 2.8 cm that occurs among the *Neogastroplites*, an oxycone would need to go ten times its body length to generate as little drag as would a discocone (based on *Sphenodiscus* and *Scaphites* results from Jacobs 1992). The *Neogastroplites* shells with diameters greater than 10 cm ($n = 14$) are all oxycones, and would need to go only a fraction of their shell length per second to generate less drag than discocones. Though extensive data are not included in the study, the *Metengonoceras* figured in Yacobucci (2004) are about 7–12 cm. Theoretically a *Metengonoceras* with a 10-cm shell traveling one shell length per second could be expected to produce about the same drag as a discoconic *Neogastroplites* going only about one shell length per second, meaning that the *Metengonoceras* would have more efficient locomotion, and could travel farther in the same jet burst, whether dodging predators or capturing prey. Before the arrival of the epeiric interloper, *Neogastroplites* shells produced oxycones at all sizes and culminated in few very large, and likely very efficient, oxycones. After arrival of the *Metengonoceras*, the *Neogastroplites* survived with shells of discocone and even cadicone shapes, while still reaching oxyconic shapes at the largest sizes, introducing significant ontogenetic trajectory toward oxycones. Applying a fairly simple restriction to the plastic growth plan may have had a substantial paleoecological consequence. Regulation limiting development of shape to specific sizes may have allowed later species of *Neogastroplites* advanced hydrodynamic efficiency across the full variety of shells expressed, even if their musculature and metabolism did not simultaneously evolve any greater capacity for jet propulsion.

Conclusions

Comparing the results of hydrodynamic experiments and fossil data studies in Westermann Morphospace, valuable insights are gained about ammonoid response to selective pressures and shape change through time. Oxyconic and discoconic forms are producers of minimal drag at high and low Re, respectively, supporting Westermann's interpretations of the importance of variation in hydrodynamic efficiency between different shell morphotypes. If drag is a first-order selective pressure, then oxycones would be expected to be encountered among larger shells, which could be ecologically critical for short-range rapid propulsion (not necessarily persistent high-speed transport). The absence of large oxyconic and the prevalence of large serpenticonic ammonites in the earliest Jurassic suggest that hydrodynamics were not a first-order environmental pressure in the aftermath of the Triassic–Jurassic extinction. In contrast, the Cretaceous *Neogastroplites* began to favor more efficient shapes at both small (discoconic) and large (oxyconic) sizes when faced with competitive pressure from interloper *Metengonoceras*.

Comparing even the scant data available from past hydrodynamic experiments demonstrates how many factors of shell hydrodynamics are still ripe for further experimentation. The variations in shell drag due to basic geometry, ornamentation, and soft tissue behavior (including jet pulse rhythm) are critical, as well as considerations of buoyancy and stability. Comparing shell data in Westermann Morphospace easily illustrates changes in different recognized morphotype production through time. Combining the preliminary understanding of drag variation with case studies of ammonoid shell variation (both across taxa and within populations) allows estimation of specific speeds that would need to be traveled to make certain shells more efficient than others, and highlights the critical importance of shell size in morphometric studies.

Acknowledgments Thanks to M. Foote and A. Allam and a generously thorough anonymous reviewer for discussions and suggested improvements on the manuscript. Thanks to J. Chamberlain, D. Jacobs, P. Smith, and M. Yacobucci for publication and discussion of their data. Thanks especially to editors C. Klug, R. Hoffman, and D. Fuchs for helpful criticisms and for organizing the Cephalopods Past and Present meeting. Great admiration and thanks to G. E. G Westermann for patient and detailed correspondence and encouragement. This research was funded by NASA Exobiology (NNX10AQ44G).

References

Akima, R. (2013). Fortran code by H. Akima R port by Albrecht Gebhardt aspline function by Thomas Petzoldt <thomas.petzoldt@tu-dresden.de> interp2xyz, enhancements and corrections by Martin Maechler (2013). akima: Interpolation of irregularly spaced data. R package version 0.5-11. http://www.CRAN.R-project.org/package=akima.

Arkell, W. J., Frunish, W. M., Kummel, B., MIller, A. K., Moore, R. C., Shindewolf, O. H., Sylvester-Bradley, P. C., & Wright, W. C., 1957, *Mollusca 4, Cephalopoda, Ammonoidea.* New York: Geological Society of America.

Chamberlain, J. (1976). Flow patterns and drag coefficients of cephalopod shells. *Palaeontology, 19*, 539–563.

Chamberlain, J. A. (1980). The role of body extension in cephalopod locomotion. *Palaeontology*, *23*, 445–461.

Chamberlain, J. A. (1981). Hydromechanical design of fossil cephalopods. In: M. R. House, & J. R. Senior (Eds.) The Ammonoidea Special (vol. 18, pp. 289–336). London: Systematics Association

Chamberlain, J. A., Jr, & Westermann, G. (1976). Hydrodynamic properties of cephalopod shell ornament. *Paleobiology*, *2*, 316–331.

Dera, G., Neige, P., Dommergues, J.-L., Fara, E., Laffont, R., & Pellenard, P. (2010). High-resolution dynamics of early Jurassic marine extinctions: the case of Pliensbachian-Toarcian ammonites (Cephalopoda). *Journal of the Geological Society, 167*, 21–33.

Dommergues, J.-L., Laurin, B., & Meister, C. (2001). The recovery and radiation of early Jurassic ammonoids: morphologic versus palaeobiogeographical patterns. *Palaeogeography, Palaeoclimatology, Palaeoecology, 165*, 195–213.

Dommergues, J.-L., Montuire, S., & Neige, P. (1996). Evolution of ammonoid morphospace during the early Jurassic radiation. *Paleobiology, 22*, 219–240. doi:10.1666/0094-8373(2002)028<0423:SPTTTC>2.0.CO;2.

Elmi, S. (1991). Données expérimentales sur l'architecturefonctionnelle de la coquille des ammonoides jurassiques. *Geobios, 13*, 155–160.

Elmi, S. (1993). Loi des aires, couche-limite et morphologie fonctionnelle de la coquille des céphalopodes (ammonoidés). *Geobios, 15*, 121–128.

Guex, J. (1995). Ammonites hettangiennes de la Gabbs Valley Range (Nevada, USA). *Mémoires De Géologie Lausanne, 27*, 1–131.

Guex, J. (2001). Environmental stress and atavism in ammonoid evolution. *Eclogae Geologicae Helvetiae*, *94*, 321–328.

Guex, J. (2003). A generalization of Cope's rule. *Bulletin de la Société géologique de France*, *174*, 449–452.

Guex, J. (2006). Reinitialization of evolutionary clocks during sublethal environmental stress in some invertebrates. *Earth and Planetary Science Letters*, *242*, 240–253.

Hammer, O., & Bucher, H. (2006). Generalized ammonoid hydrostatics modelling, with application to Intornites and intraspecific variation in Amaltheus. *Paleontological Research, 10*, 91–96. doi:10.2517/prpsj.10.91.

Hone, D., & Benton, M. (2005). The evolution of large size: how does Cope's rule work? *Trends in Ecology and Evolution, 20*, 4–6.

Jacobs, D. (1992). Shape, drag, and power in ammonoid swimming. *Paleobiology, 18*, 203–220.

Jacobs, D. K., Landman, N. H., & Chamberlain, J. A. (1994). Ammonite shell shape covaries with facies and hydrodynamics: iterative evolution as a response to changes in basinal environment. *Geology, 22*, 905–908.

Klug, C., & Korn, D. (2004). The origin of ammonoid locomotion. *Acta Palaeontologica Polonica*, *49*, 235–242.

Korn, D. (2010). A key for the description of Palaeozoic ammonoids. *Fossil Record, 13*, 5–12.

McGowan, A. J. (2004). Ammonoid taxonomic and morphologic recovery patterns after the Permian–Triassic. *Geology, 32*, 665–668.

Monnet, C., Bucher, H., Guex, J., & Wasmer, M. (2011a). Large-scale evolutionary trends of Acrochordiceratidae Arthaber, 1911 (Ammonoidea, Middle Triassic) and Cope's rule. *Palaeontology, 55*, 87–107. doi:10.1111/j.1475-4983.2011.01112.x.

Monnet, C., De Baets, K., & Klug, C. (2011b). Parallel evolution controlled by adaptation and covariation in ammonoid cephalopods. *BMC Evolutionary Biology, 11*, 115. doi:10.1186/1471-2148-11-115.

Olóriz, F., Palmqvist, P., & Pérez-Carlos, J. A. (1997). Shell features, main colonized environments, and fractal analysis of sutures in Late Jurassic ammonites. *Lethaia, 30*, 191–204.

Olóriz, F., Palmqvist, P., & Pérez-Carlos, J. A. (2002). Morphostructural constraints and phylogenetic overprint on sutural frilling in Late Jurassic ammonites. *Lethaia, 35*, 158–168.

Raup, D.M., (1967). Geometric analysis of shell coiling: coiling in ammonoids. *Journal of Paleontology,* p. 43–65.

R Core Team, (2013). R: a language and environment for statistical computing. R Foundation for Statistical Computing, Vienna, Austria. http://www.R-project.org/.

Ritterbush, K. A., & Bottjer, D. J. (2012). Westermann Morphospace displays ammonoid shell shape and hypothetical paleoecology. *Paleobiology,*. doi:10.1666/10027.1.

Saunders, W. B., & Shapiro, E. A. (1986). Calculation and simulation of ammonoid hydrostatics. *Paleobiology, 12*, 64–79.

Schaltegger, U., Guex, J., Bartolini, A., Schoene, B., & Ovtcharova, M. (2008). Precise U–Pb age constraints for end-Triassic mass extinction, its correlation to volcanism and Hettangian post-extinction recovery. *Earth and Planetary Science Letters*, *267*, 266–275.

Schoene, B., Guex, J., Bartolini, A., Schaltegger, U., & Blackburn, T. J. (2010). Correlating the end-Triassic mass extinction and flood basalt volcanism at the 100 ka level. *Geology*, *38*, 387–390.

Selden, P. A. (2009). Mollusca 4, vol. 2. Carboniferous and Permian Ammonoidea: Part L (Revised). In: R. C. Moore (Ed.), *Treatise on invertebrate paleontology*. Lawrence: Geological Society of America, Boulder, Colo., and University of Kansas.

Simon, M. S., Korn, D., & Koenemann, S. (2011). Temporal patterns in disparity and diversity of the Jurassic ammonoids of southern Germany. *Fossil Record, 14*, 77–94.

Smith, P.L., (1986). The implications of data base management systems to paleontology: a discussion of Jurassic ammonoid data. *Journal of Paleontology,* p. 327–340.

Smith, P. L., Longridge, L. M., Grey, M., Zhang, J., & Liang, B. (2014). From near extinction to recovery: Late Triassic to Middle Jurassic ammonoid shell geometry. *Lethaia, 47*, 337–351. doi:10.1111/let.12058.

Smith, P. L., & Tipper, H. W. (1986). Plate tectonics and paleobiogeography: early Jurassic (Pliensbachian) endemism and diversity. *Palaios, 1*, 399–412.

Venables, W. N., & Ripley, B. D. (2002). *Modern applied statistics with S* (4th ed.). New York: Springer. ISBN 0-387-95457-0.

Westermann, G. E. G., (1996). Ammonoid life and habitat. In: N. Landman, K. Tanabe, R. A. Davis (Eds.), *Ammonoid paleobiology* (pp. 607–707). New York: Plenum Press.

Westermann, G. E. G., & Tsujita, C. J. (1999). Life Habits of Ammonoids, chap. 21. In: E. Savazzi, (Ed.), *Functional Morphology of the Invertebrate Skeleton* (pp. 299–325). Chichester: Wiley.

Yacobucci, M. M. (2004). Neogastroplites meets Metengonoceras: morphological response of an endemic hoplitid ammonite to a new invader in the mid-Cretaceous Mowry Sea of North America. *Cretaceous Research, 25*, 927–944. doi:10.1016/j.cretres.2004.09.001.